

# Comparison of Dipolar, H-Bonding, and Dispersive Interactions on Gelation Efficiency of Positional Isomers of Keto and Hydroxy Substituted Octadecanoic Acids

Amrita Pal,<sup>†,§</sup> Shibu Abraham,<sup>†,‡</sup> Michael A. Rogers,<sup>||</sup> Joykrishna Dey,<sup>§</sup> and Richard G. Weiss<sup>\*,†,‡</sup>

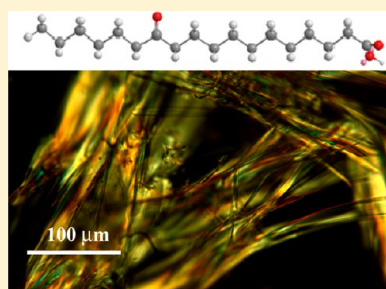
<sup>†</sup>Department of Chemistry and <sup>‡</sup>Institute for Soft Matter Synthesis and Metrology, Georgetown University, Washington, D.C. 20057-1227, United States

<sup>§</sup>Department of Chemistry, Indian Institute of Technology Kharagpur, Kharagpur 721302, India

<sup>||</sup>Department of Food Science, Rutgers University, The State University of New Jersey, New Brunswick, New Jersey 08901, United States

## S Supporting Information

**ABSTRACT:** A systematic study of the importance of functional group position and type on the gelator efficiencies of structurally simple, low molecular-mass gelators is reported. Thus, the gelation abilities of a series of positional isomers of ketoctadecanoic acid (*n*-KSA) are compared in a wide range of liquids. The gelation abilities of the *n*-KSA as a function of *n*, the keto group position along the chain, are characterized by several structural, thermal, and rheological techniques and are compared with those of the corresponding hydroxyoctadecanoic acid isomers (*n*-HSA) and the parent molecule, octadecanoic acid (SA). Analyses of the gels according to the strengths of functional group interactions along the alkyl chain in terms of group position and type are made. The conclusions derived from the study indicate that gel stability is enhanced when the functional group is located relatively far from the carboxylic headgroup and when group–group interactions are stronger (i.e., hydrogen-bonding interactions are stronger in the *n*-HSA than dipole interactions in the *n*-KSA, which are stronger than the London dispersion interactions in SA). Co-crystals of the keto- and hydroxy-substituted octadecanoic acids are found to be less efficient gelators than even the ketoctadecanoic acids, due to molecular packing and limited group interactions within the gelator networks.



## INTRODUCTION

Low-molecular-weight organogelators (LMOGs) have received considerable interest during the past few years.<sup>1–10</sup> They afford insights into one-dimensional (1D) and 3-dimensional (3D) assembly processes, as well as providing many realized and potential applications in fields such as drug delivery,<sup>11–14</sup> tissue engineering,<sup>15–17</sup> syntheses of nanomaterials and devices,<sup>18–24</sup> sensing,<sup>25</sup> and soft lithography.<sup>26</sup> LMOGs self-assemble frequently into 3D fibrillar networks (SAFINs) as a consequence of a variety of noncovalent interactions, such as London dispersion forces, van der Waals forces, hydrogen bonding (H bonding), and electrostatic and interfacial attractions or repulsions.<sup>27–29</sup> Among the 1D units, other than fibrillar objects which have been observed for the self-assembly, are platelets (which are 2D on the micrometer scale) and nanotubes. The 3D networks, formed when the aggregates interact, are able to entrap and immobilize large volumes of the liquid components by surface tension and capillary forces.<sup>30</sup>

(*R*)-12-Hydroxyoctadecanoic acid [or (*R*)-12-hydroxystearic acid; (*R*)-12-HSA] is a naturally occurring molecule that can be extracted in large quantities from castor beans.<sup>31</sup> 12-HSA and several of its related salts are known to form gels in a variety of organic liquids,<sup>32–34</sup> and semisolid dispersions of lithium salts of 12-HSA in oils have been used in the lubrication

industry.<sup>35,36</sup> The racemic mixture of enantiomers of 12-HSA also forms gels,<sup>37</sup> although much less efficiently than the enantiopure form. The difference between the two can be traced to the nature of their aggregates in the gels: optically pure 12-HSA forms fibrils, whereas the racemate forms platelets, which are more difficult to transform into strong 3D networks.<sup>38</sup> Also, the self-assembly and gelation of positional isomers of racemic hydroxyoctadecanoic acids (*n*-HSA), in which the position of the hydroxy group is unchanged but the position of the hydroxy group is moved to different positions, *n*, along the alkyl chains, have been investigated to determine the importance of the location of the hydroxy group in the self-assembly process.<sup>39</sup>

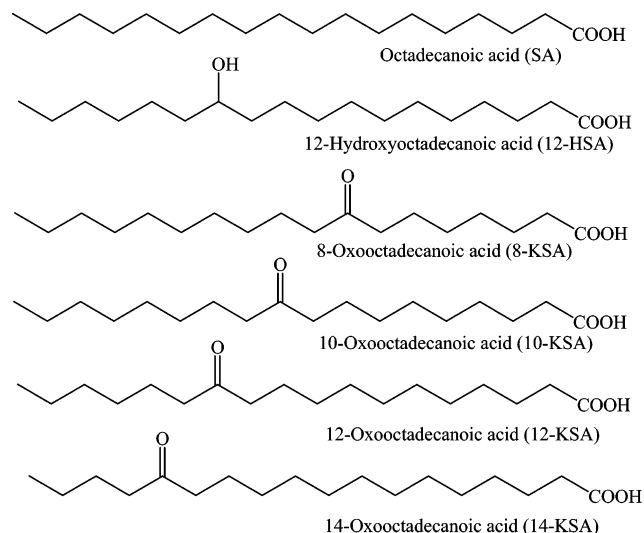
In this work, we report the gelation behavior of a series of oxooctadecanoic acids (*n*-KSA), which are easily synthesized from their respective *n*-HSA (Chart 1). The KSA have no chiral centers, and their keto–keto dipolar interactions are expected to be much weaker than the H-bonding interactions experienced by their racemic *n*-HSA analogues—a better basis for comparison than the enantiomerically pure *n*-HSA—but

Received: February 20, 2013

Revised: April 12, 2013

Published: May 14, 2013

**Chart 1. Structure of Stearic Acid (SA), 12-Hydroxyoctadecanoic Acid (12-HSA) and Positional Isomers of *n*-KSA Investigated Here**



stronger than the London dispersion forces between two CH<sub>2</sub> groups on octadecanoic acid [stearic acid (SA)], the parent molecule with no substituent along the alkyl chain. Typical intermolecular H-bonding interactions can be >10 kcal/mol, whereas dipole–dipole forces are usually <3 kcal/mol and London forces amount to no more than 2 kcal/mol. However, calculations indicate that properly oriented carbonyl–carbonyl dipolar interactions with ca. 3 Å intergroup C–O separations can be worth >5 kcal/mol,<sup>40</sup> nearly as stabilizing as many H bonds. Of course, changes in molecular volumes and conformations caused by the keto and hydroxy groups must be considered along with these attractive interactions when assessing the influence of the various functional groups on their ability to affect aggregation and gelation. From the incremental method of Bondi,<sup>41,42</sup> the group volumes of CH<sub>2</sub>, CH(OH), and C=O are 10.23, 14.82, and 11.70 cm<sup>3</sup>/mol, respectively. Thus, the C=O group is very similar in size to a CH<sub>2</sub>, although the C–C–C bond angles at the point of substitution differ. In fact, the disturbing influence of the group with the largest group volume, CH(OH), can be most easily offset by H-bonding attractions.

With consideration of these factors, albeit qualitatively, this investigation allows the relative strengths of interactions by methylene–methylene (i.e., London dispersion forces), hydroxy (i.e., H bonding), and keto (i.e., dipole–dipole forces) groups along the alkyl chain of SA to be compared in a rational manner with regard to their self-assembly and action as LMOGs. The gels have been characterized by polarizing optical microscopy, X-ray diffraction, differential scanning calorimetry, and rheology measurements. The gelation behaviors of 1:1 mixtures of *n*-KSA and *n*-HSA have also been investigated to determine whether cocrystals can be made and, if so, their relative abilities to promote gelation.

## EXPERIMENTAL SECTION

**Materials.** (*R*)-12-Hydroxystearic acid, the *D*-enantiomer (Arizona Chemical), was purified by 3 recrystallizations from a 1:19 ratio of ethyl acetate:hexane to yield a white solid, mp 78.5–81.5 °C (lit 78.5–80.8 °C).<sup>34</sup> The other *n*-HSA, 8-hydroxyoctadecanoic acid, 10-hydroxyoctadecanoic acid, and 14-hydroxyoctadecanoic acid are racemic and were available from a previous study. Methyl 12-

oxooctadecanoate (Arizona Chemical), mp 48.5–52 °C (lit. 57.1 °C)<sup>43</sup> was used as received in subsequent syntheses. Acetone (Sigma-Aldrich, HPLC grade), Na<sub>2</sub>Cr<sub>2</sub>O<sub>7</sub>·2H<sub>2</sub>O (J.T. Baker, >99%), conc. H<sub>2</sub>SO<sub>4</sub> (Mallinckrodt, >95%), dimethyl sulfoxide (DMSO, Fischer, 99.9%), KOH (Sigma-Aldrich), and ethanol (The Warner Graham Company, 190 proof) were used as received.

**Syntheses.** 12-HSA (3.0 g, 10 mmol) was added to a stirred solution of Na<sub>2</sub>Cr<sub>2</sub>O<sub>7</sub>·2H<sub>2</sub>O (2.10 g, 7.00 mmol) in DMSO (3 mL). Conc. H<sub>2</sub>SO<sub>4</sub> (2.00 g, 2.50 equiv) was added dropwise with stirring, maintaining the temperature below 80 °C. The mixture was heated and stirred at 70 °C for 2 h and stirred for an additional 12 h at room temperature. The reaction mixture was poured into ice-cold water, and the solid that precipitated was filtered. The solid was passed through a silica gel column using 1:9 ethyl acetate:hexane as the eluent and finally recrystallized from acetone to obtain 12-oxooctadecanoic acid as a white solid. The other *n*-KSA were synthesized by similar methods.

**8-KSA.** Yield: 64%. Mp: 78.9–81.5 °C. <sup>1</sup>H NMR (CDCl<sub>3</sub>, 400 MHz): δ 0.86–0.88 (m, 3H), 1.26–1.63 (m, 24H), 2.33–2.38 (m, 6H). Elemental analysis: Calcd %, C 72.48, H 11.40; Obsd %, C 72.30, H 11.79.

**10-KSA.** Yield: 29%. Mp: 78.9–81.8 °C. <sup>1</sup>H NMR (CDCl<sub>3</sub>, 400 MHz): δ 0.89–0.92 (m, 3H), 1.26–1.62 (m, 24H), 2.33–2.38 (m, 6H). Elemental analysis: Calcd %, C 72.48, H 11.40; Obsd %, C 72.91, H 11.56.

**12-KSA.** Yield: 26%. Mp: 79.1–81.7 °C (lit value 78.7–81.4 °C).<sup>34</sup> <sup>1</sup>H NMR (CDCl<sub>3</sub>, 400 MHz): δ 0.89–0.92 (m, 3H), 1.27–1.61 (m, 24H), 2.33–2.38 (m, 6H). IR (KBr, cm<sup>-1</sup>): 2914, 2849, 1696, 1469, 1440, 1381, 1341, 1294, 1278, 1223, 1209, 1130, 1073, 1025, 992, 919, 861, 830, 719, 685, 625. Elemental analysis: Calcd %, C 72.48, H 11.40; Obsd %, C 72.41, H 11.70.

**14-KSA.** Yield: 30%. Mp: 79.8–81.6 °C. <sup>1</sup>H NMR (CDCl<sub>3</sub>, 400 MHz): δ 0.86–0.89 (m, 3H), 1.27–1.64 (m, 24H), 2.35–2.38 (m, 6H). Elemental analysis: Calcd %, C 72.48, H 11.40; Obsd %, C 72.38, H 11.66.

**Instrumentation.** <sup>1</sup>H NMR spectra in CDCl<sub>3</sub>, using tetramethylsilane as the internal standard, were recorded on a Varian 400 MHz spectrometer by averaging 256 FIDs and were analyzed with VnmfJ. IR spectra were recorded on a Perkin-Elmer Spectrum One Fourier-transform-infrared (FT-IR) spectrometer. Elemental analyses were carried out on a Perkin-Elmer PE2400 microanalyzer using acetanilide as a calibration standard; reported values are averages of 3 measurements. Melting points and polarizing optical micrographs (POMs) were acquired using a Leitz 585 SM-LUX-POL microscope equipped with crossed polarizers, a Leitz 350 heating stage, a Photometrics CCD camera interfaced to a computer, and an Omega HH503 microprocessor thermometer connected to a J-K-T thermocouple. The samples for POM were flame-sealed in 0.4 or 0.5 mm path length, flattened Pyrex capillary tubes (VetroCom) heated to their solution/sol phase in a boiling water bath and cooled in a slow or fast cooling process (defined later under Gelation and Gel Melting Temperature Measurements).

Powder X-ray diffraction (XRD) patterns of samples sealed in 1 mm glass capillaries (W. Müller, Schönwalde, Germany) were obtained on a Rigaku R-Axis image plate system with Cu Kα X-rays (λ = 1.54 Å) generated by a Rigaku generator operating at 40 kV and 30 mA with the collimator at 0.5 mm (to obtain 0.5 mm diameter beams of X-rays). Data processing and analyses were performed using the Materials Data JADE (version 5.0.35) XRD pattern processing software. Diffraction data were collected for 2 h for neat powders and 10 h for gels. Diffraction data of the solvents used for measuring the XRD of the gels were also collected for 10 h and then were subtracted empirically from the diffractograms of the gels.<sup>44</sup>

Differential scanning calorimetry (DSC) measurements were made using a TA Instruments model Q200 calorimeter. Neat samples (~2–5 mg) were sealed in Tzero aluminum pans, heated to 100 °C for 2 min, and cooled at 5 °C/min to 25 °C. After 5 min at this temperature, the samples were heated at 10 °C/min to 100 °C. Organogel samples (~7–11 mg) were sealed in Tzero aluminum pans, heated at 100 °C, and then cooled to 25 °C at a rate of 5 °C/min for three heating–cooling cycles.

Rheological measurements were performed on an Anton Paar Physica MCR 301 rheometer equipped with Peltier temperature-controlled parallel plates (25 mm diameter, 0.5 mm gap) and a solvent trapping device (to minimize evaporation of the liquid during measurements). Data were collected using Rheoplus/32 Service version 3.10 and analyzed to obtain the storage modulus  $G'$  (a measure of elasticity) and loss modulus  $G''$  (a measure of viscosity), as a function of time. The sol–gel transformation was performed in situ between two 25 mm (diameter) plates with a gap of 0.5 mm. Initially, an aliquot of gel was placed on the lower plate (heated at 80 °C), and the upper plate was lowered. The plates were heated to 90 °C and kept at that temperature for 2 min. Then, the system was cooled to 25 °C at a rate of 5 °C/min. Three aliquots of each sample were run.

Some samples in glass tubes that did not form gels when shaken by hand were sonicated for about 1 min by placing them in a water bath in a Branson model 1210 sonicator. None formed a gel after this procedure (*vide infra*).

**Gelation and Gel Melting Temperature Measurements.** Gel melting temperatures were determined by the inverse flow method (i.e., the temperature ranges over which a gel fell under the influence of gravity when inverted in a sealed glass tube (5 mm i.d.) that was placed in a water bath, which was heated from room temperature at ca. 1.5 °C/min).<sup>45</sup> The initial gelator concentrations were 5%; throughout, % concentrations are in gelator weight/liquid weight ratios. Then, small weighed aliquots of the liquid component were added incrementally until no gel was evident by the falling drop method<sup>46</sup> (i.e., heating slowly an inverted sample in a sealed tube and noting the range over which the gel begins and then completely falls) at room temperature. After the addition of each liquid aliquot, the tube was resealed and the gel was reformed as explained above.

Both slow- and fast-cooling protocols were used to convert the hot solutions/sols to gels. In the slow-cooling protocol, weighed amounts of a *n*-KSA and a liquid in a sealed tube were heated in a water bath until the LMOG dissolved completely (i.e., a transparent sol was formed), the heating unit was removed, and the sol was cooled at a nonlinear rate (~50 °C/h) in the water bath until it reached room temperature. In the fast-cooling protocol, the hot sol, prepared as before, was immediately placed in an ice bath for several minutes. In both cases, the sol was kept at the elevated temperature for about 2 min and then allowed to cool without any mechanical agitation.

## RESULTS AND DISCUSSION

**Gelation Behavior.** Screening studies of the gelating ability of 5% of the *n*-KSA were conducted in a wide range of organic liquids (Table 1). The phase designations are based on qualitative visual assessments. Data for critical gelator concentrations (CGCs) are collected in Table 2; they will be discussed later. All of the *n*-KSA were insoluble in water even at its boiling point, and very similar results were obtained with the slow- and fast-heating protocols (*vide ante*). In those samples where partial gelation or precipitation was observed, they were sonicated at room temperature for about 1 min, heated to 90 °C until a clear sol was observed, and then cooled to room temperature by both the slow- and fast-cooling methods. This procedure led to the same final morphologies as found without sonication: no gels were formed.

Packing within fibers of a SAFIN is controlled by a balance among physical interactions, such as London dispersion forces, intermolecular H bonding, electrostatic forces, and  $\pi$ – $\pi$  stacking.<sup>47</sup> The only important stabilizing interaction available within the fibers of *n*-alkanes is London dispersion forces. Because each CH<sub>2</sub>/CH<sub>2</sub> interaction is worth ~2 kcal/mol,<sup>48</sup> their sum within lamellae of long *n*-alkanes is substantial, allowing the network to immobilize liquids. Stearic acid (SA) offers additional interactions from H bonding between carboxylic acid groups within the LMOG assemblies. In that regard, when cooled below a characteristic temperature ( $T_{gs}$ ),

**Table 1. Gelation Behavior<sup>a</sup> of 5% of the *n*-KSA and 2% HSA<sup>45</sup> in a Wide Range of Liquids**

	8-KSA	10-KSA	12-KSA	14-KSA	HSA
hexane	P	P	WG	WG	OG
cyclohexane	PG	OG	OG	OG	–
<i>n</i> -decane	OG	OG	OG	OG	OG
benzene	STG	OG	OG	OG	CG
toluene	WG	PG	PG	PG	CG
acetone	P	P	P	P	–
CH <sub>2</sub> Cl <sub>2</sub>	S	S	S	S	–
CHCl <sub>3</sub>	S	S	S	S	OG
CCl <sub>4</sub>	OG	WG	WG	WG	CG
methanol	S	S	S	S	S
ethanol	S	S	S	S	–
1-octanol	PG	PG	PG	PG	S
DMF	S	S	S	S	–
DMSO	DS	DS	DS	DS	S
acetonitrile	PG	PG	PG	PG	OG
water	I	I	I	I	I
safflower oil	VS	VS	VS	VS	–
silicone oil	OG	OG	OG	OG	OG

<sup>a</sup>S = clear solution; I = insoluble; P = precipitate; PG = partial gel; OG = opaque gel; WG = weak gel; STG = semitransparent gel, DS = dispersion, VS = viscous solution, CG = clear gel.

**Table 2. CGC Values (%) of *n*-KSA and of a 1:1 Ratio of *n*-KSA:*n*-HSA Mixtures**

LMOG	mineral oil	silicone oil	decane
8-KSA	3.2	1.2	3.8
10-KSA	2.9	1.6	3.6
12-KSA	2.5	1.4	3.7
14-KSA	0.6	1.1	3.9
1:1 8-KSA:8-HSA	2.9	1.0	
1:1 10-KSA:10-HSA	2.4	1.2	
1:1 12-KSA:12-HSA	1.9	1.0	3.1
1:1 14-KSA:14-HSA	1.7	0.9	

solutions of relatively high concentrations of long-chained saturated fatty acids and their salts are known to form gelatinous materials with fibrous structures.<sup>49–51</sup> However, at 2% concentrations of SA, none of the samples with decane, silicone oil, CCl<sub>4</sub>, toluene, or acetonitrile as the liquid produced a gel.<sup>45</sup> The introduction of a hydroxyl group along the alkyl chain of SA, as in *n*-HSA, can change the gelating ability of an LMOG enormously. In the most impressive indirect structural determination of LMOG packing in gels, Terech et al. found that X-ray diffractograms of the organogels, aerogels, and crystalline powders of either chiral or racemic 12-HSA have almost the same structural features.<sup>37</sup> Unfortunately, a single crystal X-ray analysis of neither chiral nor racemic 12-HSA could be obtained. However, peaks in the XRD pattern that characterize the crystalline nature of the network structure could be correlated with X-ray diffractograms of structurally related compounds, such as SA, whose single crystal structures are known.<sup>52–55</sup> Subsequent studies by Rogers and co-workers demonstrated that the plateletlike and fiberlike aggregates of racemic and enantiopure *n*-HSA can be traced to subtle differences in the modes of the hydroxy–hydroxy interactions.<sup>56</sup>

As expected on the basis of the relative strengths of potential H-bonding and dipolar keto-group interactions, the optically

pure *n*-HSA are more efficient gelators than the *n*-KSA.<sup>45,48</sup> For example, 2% (*R*)-12-HSA can gelate a large number of organic liquids,<sup>45</sup> but 2% 12-KSA can gelate only silicone oil, mineral oil, and *n*-decane (of the liquids examined). In general, the gels of the *n*-HSA are stronger than those of the corresponding *n*-KSA (using CGCs, temperatures of gelation, and diversity of liquids gelated at the same concentrations as the criteria). These results follow the strengths of the 3D network formed by *n*-KSA and *n*-HSA based upon their heats of melting from DSC measurements.

Although both the *n*-KSA and *n*-HSA experience lipophilic interactions along their long alkyl chains, the 3D networks of the *n*-HSA can, in principle, derive additional strength from the H-bonding interactions between hydroxyl groups that are not matched in strength by the dipole–dipole keto-group interactions in the *n*-KSA. Of the CGC values for the gels formed by the *n*-KSA (Table 2), those with silicone oil are the lowest (implying that they are also the strongest). Also, all of the *n*-KSA gels with silicone oil and mineral oil near the CGCs were translucent at room temperature.

To investigate further the effect of H bonding on the efficiency of gelation, 1:1 mixtures of 5% total gelator concentrations of 12-HSA and 12-KSA were examined in water and some organic solvents. A new complex, formed by the mixture, gelated only decane, mineral oil, and silicone oil completely (opaque gels). When these samples, although only partially gelated, were sonicated as described in the Experimental Section, they remained either partial gels or precipitates.

**Morphology.** The appearances of the SAFINs of 5% *n*-KSA gels in *n*-decane (Figure S1 of the Supporting Information) and in mineral oil (Figure 1) at the micrometer spatial range depended on the protocol for cooling the sols. Larger spherulites were observed after the solutions/sols were treated by the slow-cooling protocol.<sup>53–56</sup> Generally, fast cooling results in a higher degree of super saturation and faster nucleation and growth (resulting, here, in short fibers or small spherulites), whereas the slow-cooled gels are composed of long, rodlike fibers.<sup>30</sup> Previously, we determined that the networks of racemic 12-HSA (as well as the other racemic *n*-HSA) in mineral oil consist of platelets, whereas (*R*)-12-HSA forms fibers.<sup>48–56</sup> By contrast, the *n*-KSA, with no chiral centers, provide only fibrous structures upon slow cooling and spherulitic objects upon fast cooling of their solutions/sols. Furthermore, the POM images of the gels in *n*-decane are similar in appearance to the gels in mineral oil (Figure 1). On the basis of the observations that homochiral interactions among OH groups of chiral *n*-HSA lead to an extended secondary stabilizing network (and assist the formation of long fibers), while the orientations of OH groups of racemic *n*-HSA do not (and orthorhombic platelets are obtained<sup>56</sup>), we conjecture that the keto–keto interactions among aggregates of the (achiral!) *n*-KSA inhibit the sorts of networks that lead to platelets and allow fiber formation.

X-ray diffraction patterns of the neat powders of the 14-KSA and their 5% fast-cooled silicone oil and mineral oil gels have been compared (Figure S2 of the Supporting Information). The diffraction peaks of the gels were identified by empirically subtracting the amorphous scattering of silicone oil or mineral oil from the total gel diffractogram.<sup>44</sup> Unfortunately, attempts to index all of the diffraction peaks and, thereby, to identify the gross natures of the cell packings were unsuccessful. On the basis of the layered packing arrangements of the *n*-HSA and

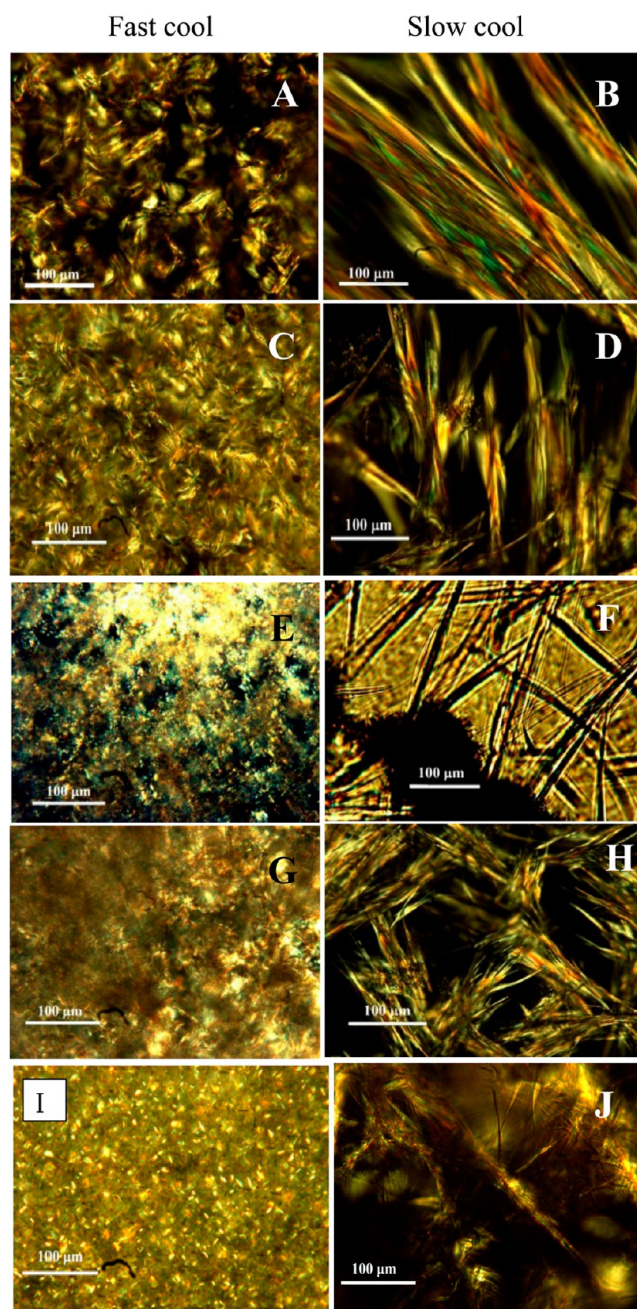


**Figure 1.** POM images of mineral oil gels containing 5% LMOG: (A and B) 8-KSA, (C and D) 10-KSA, (E and F) 12-KSA, (G and H) 14-KSA, and containing (I and J) 1:1 12-KSA:12-HSA.

many of their derivatives,<sup>45,56</sup> we assume that (except as indicated below) the molecular packing within the *n*-KSA SAFIN structures are also lamellar and that the lowest angle diffraction peaks correspond to the layer spacings ( $d$ , nm) (Table 3). These distances are compared with the length of the *n*-KSA, 2.68 nm, calculated in their completely extended conformations at the MM2 level<sup>57</sup> and adding the van der Waals radii of the terminal atoms. The bilayer thicknesses of the aggregates in the neat *n*-KSA and in their mineral oil gels are less than twice the extended molecular length. The  $d$  values of the corresponding *n*-HSA positional isomers as neat powders and in mineral oil gels, 4.3–4.8 nm, are smaller than those of the *n*-KSA, 4.7–4.8 nm. Because the extended molecular lengths of the two families are nearly the same, either the *n*-

**Table 3. Lattice Spacings ( $d$ , nm) of Neat  $n$ -KSA (Calcd Length = 2.68 nm) and a 1:1 Ratio of  $n$ -KSA: $n$ -HSA Mixtures and of the SAFINs in Mineral Oil and Silicone Oil Gels (5%) at Room Temperature**

LMOG	$d$ (nm)		
	powder	mineral oil gel	silicone oil gel
8-KSA	4.74	4.85	9.28
1:1 8-KSA:8-HSA	4.69	4.69	5.19
10-KSA	4.74	4.80	5.22
1:1 10-KSA:10-HSA	4.72	4.62	5.36
12-KSA	4.69	4.74	7.13
1:1 12-KSA:12-HSA	4.74	4.82	5.24
14-KSA	4.74	4.84	9.20
1:1 14-KSA:14-HSA	4.74	4.72	8.32

KSA are less interdigitated within bilayers, their long axes are closer to being normal to the layer planes, or they have fewer gauche bends along the chains than do the  $n$ -HSA. Also, it was observed that the thicknesses of the packing units within the fibers of some of the  $n$ -KSA gels in silicone oil are greater than twice the extended molecular length; we assume that the packing arrangements in those gels are different from the lamellar arrangements noted above.

The diffraction pattern of a 1:1 12-KSA:12-HSA mixture was different from that of neat 12-KSA or 12-HSA (Figure 3). The

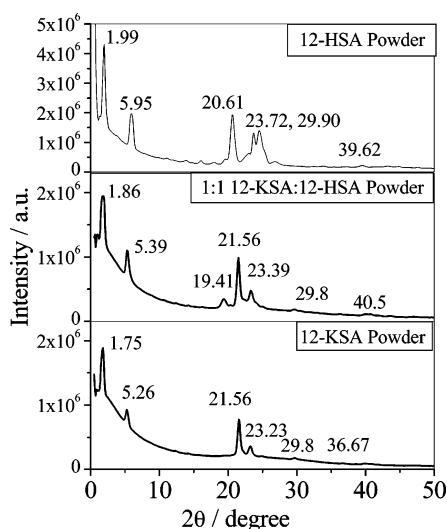


**Figure 3.** XRD patterns of neat 12-HSA, 12-KSA, and 1:1 12-KSA:12-HSA. The numbers in the panels are the diffraction angles in  $2\theta$ .

**Table 4.  $T_{gs}$  ( $^{\circ}\text{C}$ ) Values of 5% Gels of  $n$ -KSA and a 1:1 Ratio of 12-KSA:12-HSA, Prepared by the Fast-Cooling Protocol, in Different Organic Liquids**

solvent	$T_{gs}$ ( $^{\circ}\text{C}$ )					
	8-KSA	10-KSA	12-KSA	1:1 12-KSA:12-HSA	14-KSA	
cyclohexane	–	47–51	48–50	–	–	48–52
$n$ -decane	67–69	65–69	63–65	65–69	–	62–65
benzene	32–34	30–33	30–32	–	–	31–33
toluene	30–31	–	–	–	–	–
$\text{CCl}_4$	42–44	39–43	35–37	–	–	33–36
silicone oil	76–77	77–78	75–76	76–78	–	74–76
mineral oil	68–70	69–71	69–70	59–60	–	67–69

$d$  values of the mixture, 12-KSA and 12-HSA, are 4.74, 5.04, and 4.43 nm, respectively. These observations indicate that the mixture is a cocrystal, a new complex rather than a mixture of the individual crystals of 12-KSA and 12-HSA.

**FT-IR Spectra and Functional Group–Group Interactions.** FT-IR spectra of the mixture and neat components were recorded (Figure S3 of the Supporting Information) in an attempt to decipher the origin of the stability of the new complex. Although it is difficult to dissect the various peaks in the spectral regions of interest, the lower OH stretching frequency of the mixture than that of neat 12-HSA indicates the presence of a new H-bonding mode in the mixture, which probably arises from OH–carbonyl interactions, which are superimposed on the carboxylic acid OH peak.

**Thermal Stability of Gels.** Gel melting temperatures ( $T_{gs}$ ), obtained by the falling drop method, are reported in Table 4 for samples with 5% gelator concentrations (i.e., in the “plateau” regions, where the 3D networks are fully formed). They are nearly independent of the position of the keto group in the  $n$ -KSA investigated (Figure 4) and whether gels were made by

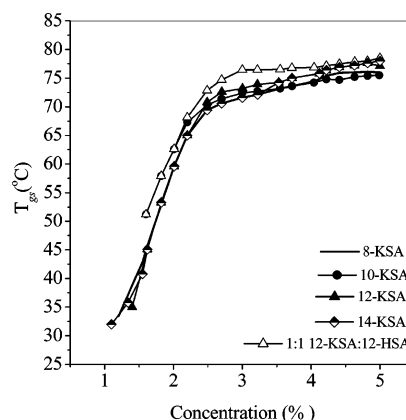


**Figure 4.** Dependence of  $T_{gs}$  on LMOG concentration in silicone oil gels.

the fast- or slow-cooling protocols; only the fast-cooling data are presented. Generally, the  $T_{gs}$  values are slightly higher for gels made by the slow-cooling process. This observation is consistent with the longer fibers found in the SAFINs of slow-cooled gels (vide ante). Although the  $T_{gs}$  values of the gels of 12-KSA in silicone oil and in  $n$ -decane are similar to those of the 12-HSA gels,<sup>44</sup> the  $T_{gs}$  values of the 12-HSA gels with the other liquids investigated were higher, indicating again that the keto–keto interactions in the 12-KSA gels are weaker than the H-bonding interactions among the hydroxyl groups of 12-HSA.

Although the  $T_{gs}$  values of the gel formed by the 1:1 mixture in *n*-decane and silicone oil are similar to those in 12-KSA, only partial or weak gels were obtained from the mixture in cyclohexane, benzene, and carbon tetrachloride. Thus, the gels with 2 gelator components appear to be very sensitive to the liquid component and are less stable, on average, than the gels prepared from neat 12-KSA; the addition of 12-HSA (and its potentially stronger H-bonding interactions) does not always lead to stronger gels.

**Mechanical Stability of Gels.** The viscoelastic properties at room temperature of the 5% mineral oil and silicone oil gels were investigated by rheology to ascertain the values of the storage modulus ( $G'$ , a measure of the strength of the gels) and the loss modulus ( $G''$ , a measure of the tendency of a material to flow under stress) (Table 5). Figures 5 and S3 show plots of

**Table 5. Critical and Crossover Strains of 5% *n*-KSA and a 1:1 Ratio of *n*-KSA:*n*-HSA Gels in Silicone Oil and Mineral Oil at 25 °C**

LMOG	liquids			
	silicone oil		mineral oil	
	critical strain	crossover	critical strain	crossover
8-KSA	0.08%	0.67%	—	—
1:1 8-KSA:8-HSA	0.10%	2.19%	—	—
10-KSA	0.13%	1.78%	—	—
1:1 10-KSA:10-HSA	0.18%	2.27%	—	—
12-KSA	0.16%	3.51%	1.30%	6.93%
1:1 12-KSA:12-HSA	0.23%	3.20%	1.60%	14.90%
14-KSA	0.19%	5.79%	0.61%	9.85%
1:1 14-KSA:14-HSA	0.23%	21.64%	1.07%	31.50%

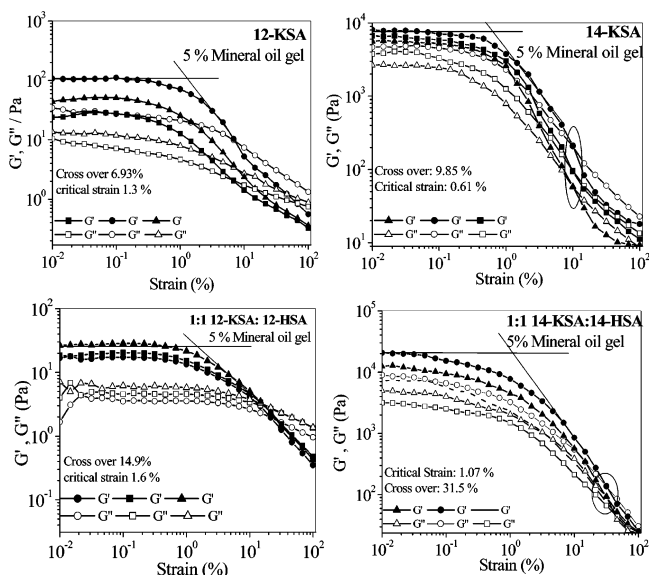


**Figure 5.** Dependence of  $G'$  and  $G''$  on applied strain for 5% 12-HSA, *n*-KSA and a 1:1 ratio of *n*-KSA:*n*-HSA gels in mineral oil at an oscillation frequency of 1 Hz and 25 °C.

$G'$  and  $G''$  versus applied strain ( $\gamma$ ) at a constant frequency of 1 Hz. Above a critical strain value ( $\gamma_c$ , the minimal strain required to partially break the network structure), both  $G'$  and  $G''$  abruptly decrease. Although  $G'$  and  $G''$  varied somewhat among 3 runs on different aliquots, the critical strain ( $\gamma_c$ ) and the

crossover point at which  $G'$  becomes equal to  $G''$  did not change.

The general trends of  $\gamma_c$  and the crossover points of the silicone oil gels (Figure S4 and Table 5) formed by 8-KSA, 10-KSA, 12-KSA, and 14-KSA indicate that the elasticity and brittleness of the gels increased as the keto group was moved farther from the carboxylic acid group. The critical strain and the crossover values of 5% silicone oil gel formed by 1:1 12-KSA:12-HSA were 0.23% and 3.20%, respectively, and those for the corresponding 12-HSA gels (Figure S5 of the Supporting Information) were 0.47% and 6.43%, respectively; by these criteria, the 12-HSA gel was stronger mechanically than the mixture gel, and it was stronger than the 12-KSA gel whose critical strain is 0.16% and crossover was 3.5%. This progression is expected on the basis of the strengths of intermolecular interactions at the 12-position.

Figure 6 and Figure S6 of the Supporting Information show the variation of  $G'$  and  $G''$  with frequency at a strain within the

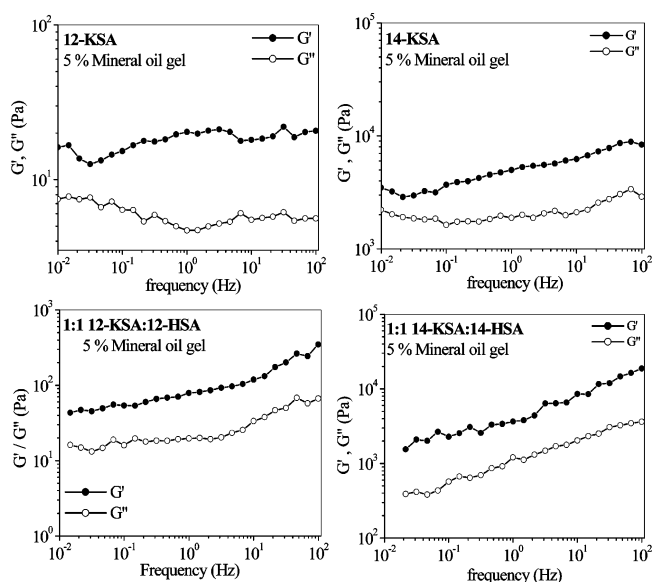


**Figure 6.** Dependence of  $G'$  (●) and  $G''$  (○) on frequency for 5% 12-HSA, *n*-KSA, and 1:1 *n*-KSA:*n*-HSA gels in mineral oil at 25 °C.

linear viscoelastic region (ranging from 0.01 to 0.1%). The observations that both  $G'$  and  $G''$  vary in a nearly parallel fashion with frequency and that  $G'$  remains higher than  $G''$  constitute good evidence that the samples are true gels.

**DSC Measurements.** The mean temperature at which a 3D network melts,  $T_m$ , and the heat associated with that transition have been measured by DSC for gels consisting of 5% *n*-KSA in silicone oil and mineral oil. The thermograms of the neat powders and gels are shown in Figure S7 of the Supporting Information and those of 1:1 *n*-KSA:*n*-HSA mixtures (powder and gel) are in shown Figures S7 and S8 of the Supporting Information. For comparison purposes, the normalized enthalpies of the transitions are listed in Table 6 to the heats associated with the melting of the neat gelators. The values reported are averages of data from second and third heating and cooling thermograms in order to avoid possible complications if the samples are not completely equilibrated initially. As expected, the  $T_m$  values of the 3D networks are always lower than the melting temperatures of their neat LMOGs; the liquid aids melting of the 3D gel networks by dissolving the molecules in the fibers over a temperature range. The lower melting

**Table 6. Melting Temperatures ( $T_m$ , °C), Crystallization Temperatures ( $T_c$ , °C), and Normalized Enthalpies ( $\Delta H$ , J g<sup>-1</sup>) of 5% LMOG in Silicone Oil and Mineral Oil Gels and Neat Solids during Their Heating and Cooling Cycles, from DSC Thermograms**

LMOG	powder				silicone oil gel				mineral oil gel			
	heating		cooling		heating		cooling		heating		cooling	
	$T_m$	$\Delta H$	$T_c$	$\Delta H$	$T_m$	$\Delta H$	$T_c$	$\Delta H$	$T_m$	$\Delta H$	$T_c$	$\Delta H$
8-KSA	83.4	4270	77.7	4150	77.9	178	69.7	172	73.1	150	69.6	164
10-KSA	81.1	4280	76.8	4130	77.5	174	70.1	158	72.9	138	68.9	7.5
12-KSA	80.4	2680	61.4	2810	78.9	148	47.1	108	71.8	130	38.5	4.6
14-KSA	82.3	3430	74.9	3520	77.2	172	66.8	188	70.9	182	56.8	10.3
1:1 8-KSA: 8-HSA	71.6	3230	60.5	3120	68.8	108	53.3	130	61.9	110	41.6	6.5
1:1 10-KSA: 10-HSA	75.5	4280	66.8	4030	67.5	164	54.1	168	62.9	128	48.9	6.5
1:1 12-KSA: 12-HSA	73.5	2910	54.1	2670	66.9	176	54.2	162	61.4	64	40.2	6.8
1:1 14-KSA: 14-HSA	67.9	3400	60.3	3230	69.5	144	52.9	150	61.1	138	40.6	7.5

temperature of the gel in mineral oil than in silicone oil indicates that the LMOGs are more easily dissolved in mineral oil. Consistent with our hypothesis that the liquid component aids in melting the 3D networks by dissolving the gelators, the normalized heats of the gel transitions are generally lower than those of the associated neat LMOG. In addition, DSC thermograms of the gels of 5% of 1:1 *n*-HSA:*n*-KSA in silicone oil and mineral oil showed lower melting (on heating) and crystallization (on cooling) temperatures, as well as smaller normalized enthalpy changes than those of the neat solid LMOGs.

The melting temperatures of gels of 2% *n*-HSA in mineral oil, 70–75 °C,<sup>56</sup> were comparable to those of the analogous *n*-KSA gels (70–73 °C) and higher than those of the 1:1 ratio of *n*-KSA:*n*-HSA gels (61–63 °C). Also, the enthalpies of melting of the *n*-KSA gels were much lower than those of the comparable *n*-HSA gels.<sup>56</sup> Again, these differences can be attributed most easily to the stronger hydroxy–hydroxy interactions within the SAFIN structures of the *n*-HSA mineral oil gels. Although 1:1 *n*-KSA:*n*-HSA mixtures do provide opportunities for stronger hydroxy-keto (than keto–keto) interactions, their extent is limited primarily to pairs of neighboring molecules (assuming an alternating arrangement of *n*-KSA and *n*-HSA molecules within a fiber). In addition, placing the *n*-KSA and *n*-HSA molecules next to each other in a mixture probably creates a substantial disturbance to local packing because the melting temperatures of even the *n*-KSA gels are higher than those of the mixture gels.

## CONCLUSIONS

The stronger functional group interactions among the keto group of the *n*-KSA enhance their gelating properties with respect to octadecanoic acid (SA) but not as well as does the introduction of a more polar hydroxyl group in the *n*-HSA series. This progression of LMOG efficiencies was expected based on the energies of the interactions between pairs of –CH<sub>2</sub>–, =C=O, and –CH(OH)– groups. The SAFINs of the gels provide one manifestation of the macroscopic differences between the *n*-KSA and *n*-HSA gels: elongated fiberlike aggregates of the achiral *n*-KSA LMOGs were formed by slow-cooling their sol phases, whereas spherulitic structures were obtained by fast-cooling the sols; regardless of the cooling protocol for the mineral oil sols, the networks of gels with racemic *n*-HSA consisted of platelets, whereas those of (*R*)-12-HSA were fibers.<sup>56</sup> However, the *n*-KSA formed true gels, albeit very weak ones.

The position of the keto functionality along the *n*-KSA chain, between *n* = 8 and *n* = 14, has little effect on the range of liquids gelled and the CGC (Table 2) and thermal stability (Table 6) of the gels. Similar trends were observed previously in the racemic *n*-HSA series as long as *n* was 6 or larger: the CGC values were found to be ca. 1.9 wt % for 6-HSA, 8-HSA, and 10-HSA and ca. 1.7 wt % for 12-HSA and 14-HSA.<sup>56</sup> Thus, placing the strongly interacting functional group, be it hydroxy or keto, closer to the carboxylic head of the molecule diminishes its stabilizing influence on its gels. From these trends, we can conclude that the conformational lability of the long alkyl chains, “pinned” at one molecular end in their aggregates by the carboxylic acid groups, are attenuated by even a keto group near the midpoint of the molecules. However, the presence of both keto- and hydroxy-containing molecules in the same aggregate causes a greater disturbance than the stabilizing influence: the packing in the immediate vicinity of the groups must be more disorganized than in the neat LMOG assemblies.

Attempts to discern the specific nature of these interactions by infrared spectroscopic and X-ray diffraction methods were of limited success. Although it is clear that the purported interactions are occurring, it is not possible to quantify their nature with the data in hand; in future experiments, perhaps a greater level of insights will be forthcoming with a synchrotron source for additional diffractions studies which is able to separate the contributions to the overall stability of the gels of group–group interaction energies and structural effects caused by the group volumes. However, even with the data in hand, it is clear that the molecular packing arrangements in the neat *n*-KSA and in their gel fibers are different in most of the samples examined; polymorphism in LMOGs is well-established in many other LMOGs.<sup>1,47</sup>

The results demonstrate the importance of the nature and the position of a keto or hydroxyl functional group along the 18-carbon atom chain of the parent molecule, octadecanoic acid, a very poor LMOG. They should be very useful to those interested in designing new or better LMOGs because the structures of the SA, *n*-HSA, and *n*-KSA are simple, containing no more than 2 functional groups on an *n*-alkane frame, and the structural variations have been systematic.

The influence of simple structural derivatizations of the carboxylic acid group of the *n*-KSA and *n*-HSA on their gelation abilities will be investigated in the future.

## ■ ASSOCIATED CONTENT

### Supporting Information

Gelation behavior, POM images, XRD of neat powders, FT-IR spectra, dependence of  $G'$  and  $G''$  on applied strain, dependence of  $G'$  and  $G''$  on frequency, and DSC thermograms. This material is available free of charge via the Internet at <http://pubs.acs.org>.

## ■ AUTHOR INFORMATION

### Corresponding Author

\*E-mail: [weissr@georgetown.edu](mailto:weissr@georgetown.edu).

### Present Address

<sup>†</sup>SBG Laboratories, Inc., 1288 Hammerwood Avenue, Sunnyvale, CA 94089, United States.

### Notes

The authors declare no competing financial interest.

## ■ ACKNOWLEDGMENTS

The U.S. National Science Foundation is gratefully acknowledged for its support of this research through Grants CHE-1147353 and CHE-0911089. A.P. thanks the Fulbright Foundation for a Fulbright-Nehru India Doctoral & Professional Research Fellowship.

## ■ REFERENCES

- (1) Terech, P.; Weiss, R. G. Low Molecular Mass Gelators of Organic Liquids and the Properties of Their Gels. *Chem. Rev.* **1997**, *97*, 3133–3160.
- (2) Abdallah, D. J.; Weiss, R. G. Organogels and Low Molecular Mass Organic Gelators. *Adv. Mater.* **2000**, *12*, 1237–1247.
- (3) Gronwald, O.; Shinkai, S. Sugar-Integrated Gelators of Organic Solvents. *Chem.—Eur. J.* **2001**, *7*, 4328–4334.
- (4) Estroff, L. A.; Hamilton, A. D. Water Gelation by Small Organic Molecules. *Chem. Rev.* **2004**, *104*, 1201–1217.
- (5) Jung, J. H.; Shinkai, S. Gels as templates for nanotubes. *Top. Curr. Chem.* **2004**, *248*, 223–260.
- (6) Sangeetha, N. M.; Maitra, U. Supramolecular gels: Functions and uses. *Chem. Soc. Rev.* **2005**, *34*, 821–836.
- (7) George, M.; Weiss, R. G. Molecular Organogels. Soft Matter Comprised of Low-Molecular-Mass Organic Gelators and Organic Liquids. *Acc. Chem. Res.* **2006**, *39*, 489–497.
- (8) Nie, X. P.; Wang, G. J. Synthesis and Self-Assembling Properties of Diacetylene-Containing Glycolipids. *J. Org. Chem.* **2006**, *71*, 4734–4771.
- (9) Yang, Z. M.; Xu, B. Using Enzymes to Control Molecular Hydrogelation. *Adv. Mater.* **2006**, *18*, 3043–3046.
- (10) Yang, Z. M.; Liang, G. L.; Xu, B. Enzymatic Hydrogelation of Small Molecules. *Acc. Chem. Res.* **2008**, *41*, 315–326.
- (11) Shirakawa, M.; Fujita, N.; Tani, T.; Kaneko, K.; Shinkai, S. Organogel of an 8-Quinololinol Platinum(II) Chelate Derivative and Its Efficient Phosphorescence Emission Effected by Inhibition of Dioxxygen Quenching. *Chem. Commun. (Cambridge, U.K.)* **2005**, 4149–4151.
- (12) Vemula, P. K.; Li, J.; John, G. Enzyme Catalysis: Tool to Make and Break Amygdalin Hydrogelators from Renewable Resources: A Delivery Model for Hydrophobic Drugs. *J. Am. Chem. Soc.* **2006**, *128*, 8932–8938.
- (13) Friggeri, A.; Feringa, B. L.; van Esch, J. H. Entrapment and Release of Quinoline Derivatives Using a Hydrogel of a Low Molecular Weight Gelator. *J. Controlled Release* **2004**, *97*, 241–248.
- (14) Tiller, J. C. Increasing the Local Concentration of Drugs by Hydrogel Formation. *Angew. Chem., Int. Ed.* **2003**, *42*, 3072–3075.
- (15) Wang, X.; Horri, A.; Zhang, S. Designer Functionalized Self-Assembling Peptide Nanofiber Scaffolds for Growth, Migration, And Tubulogenesis of Human Umbilical Vein Endothelial Cells. *Soft Matter* **2008**, *4*, 2388–2395.
- (16) Ellis-Behnke, R. G.; Liang, Y.-X.; You, S.-W.; Tay, D. K. C.; Zhang, S.; So, K.-F.; Schneider, G. E. Nano Neuro Knitting: Peptide Nanofiber Scaffold for Brain Repair and Axon Regeneration with Functional Return of Vision. *Proc. Natl. Acad. Sci. U.S.A.* **2006**, *103*, 5054–5059.
- (17) Lee, K. Y.; Mooney, D. J. Hydrogels for Tissue Engineering. *Chem. Rev.* **2001**, *101*, 1869–1879.
- (18) Li, S. C.; John, V. T.; Irvin, G. C.; Rachakonda, S. Synthesis and Magnetic Properties of a Novel Ferrite Organogel. *J. Appl. Phys.* **1999**, *85*, 5965–5967.
- (19) de Jong, J. J. D.; Lucas, L. N.; Kellogg, R. M.; van Esch, J. H.; Feringa, B. L. Reversible Optical Transcription of Supramolecular Chirality into Molecular Chirality. *Science* **2004**, *304*, 278–281.
- (20) Yagai, S.; Nakajima, T.; Kishikawa, K.; Kohmoto, S.; Karatsu, T.; Kitamura, A. Hierarchical Organization of Photoresponsive Hydrogen-Bonded Rosettes. *J. Am. Chem. Soc.* **2005**, *127*, 11134–11139.
- (21) Yang, Z. M.; Gu, H. W.; Du, J.; Gao, J. H.; Zhang, B.; Zhang, X. X.; Xua, B. Self-Assembled Hybrid Nanofibers Confer a Magneto-rheological Supramolecular Hydrogel. *Tetrahedron* **2007**, *63*, 7349–7357.
- (22) Kishimura, A.; Yamashita, T.; Aida, T. Phosphorescent Organogels via “Metallophilic” Interactions for Reversible RGB-Color Switching. *J. Am. Chem. Soc.* **2005**, *127*, 179–183.
- (23) Beck, J. B.; Rowan, S. J. Multistimuli, Multiresponsive Metallo-Supramolecular Polymers. *J. Am. Chem. Soc.* **2003**, *125*, 13922–13923.
- (24) Enomoto, M.; Kishimura, A.; Aida, T. Coordination Metallacycles of an Achiral Dendron Self-Assemble via Metal-Metal Interaction to Form Luminescent Superhelical Fibers. *J. Am. Chem. Soc.* **2001**, *123*, 5608–5609.
- (25) Xing, L.-B.; Yang, B.; Wang, X.-J.; Wang, J.-J.; Chen, B.; Wu, Q.-H.; Peng, H.-X.; Zhang, L.-P.; Tung, C.-H.; Wu, L.-Z. Reversible Sol-to-Gel Transformation of Uracil Gelators: Specific Colorimetric and Fluorimetric Sensor for Fluoride Ions. *Langmuir* **2013**, *29*, 2843–2848.
- (26) Jhaveri, S. J.; McMullen, J. D.; Sijbesma, R.; Tan, L.-S.; Zipfel, W.; Ober, C. K. Direct Three-Dimensional Microfabrication of Hydrogels via Two-Photon Lithography in Aqueous Solution. *Chem. Mater.* **2009**, *21*, 2003–2006.
- (27) Ikeda, M.; Takeuchi, M.; Shinkai, S. Unusual Emission Properties of a Triphenylene-Based Organogel System. *Chem. Commun. (Cambridge, U.K.)* **2003**, 1354–1355.
- (28) Ishi-i, T.; Hirayama, T.; Murakami, K.; Tashiro, H.; Thiemann, T.; Kubo, K.; Mori, A.; Yamasaki, S.; Akao, T.; Tsuboyama, A.; Mukaide, A. T.; Ueno, K.; Mataka, S. Combination of an Aromatic Core and Aromatic Side Chains Which Constitutes Discotic Liquid Crystal and Organogel Supramolecular Assemblies. *Langmuir* **2005**, *21*, 1261–1268.
- (29) van Esch, J.; Schoonbeek, F.; de Loos, M.; Kooijman, H.; Spek, A. L.; Kellogg, R. M.; Feringa, B. L. Cyclic Bis-Urea Compounds as Gelators for Organic Solvents. *Chem.—Eur. J.* **1999**, *5*, 937–950.
- (30) Huang, X.; Terech, P.; Raghavan, S. R.; Weiss, R. G. Kinetics of  $5\alpha$ -Cholestan- $3\beta$ -yl N-(2-naphthyl)carbamate/*n*-Alkane Organogel Formation and Its Influence on the Fibrillar Networks. *J. Am. Chem. Soc.* **2005**, *127*, 4336–4334.
- (31) Maskaev, A. K.; Man'kovskaya, N. K.; Lend'el, I. V.; Fedorovskii, V. T.; Simurova, E. I.; Terent'eva, V. N. Preparation of 12-Hydroxystearic Acid, The Raw Material for Plastic Greases. *Chem. Technol. Fuels Oils* **1971**, *7*, 109–112.
- (32) Polishuk, A. T. Properties and Performance Characteristics of Some Modern Lubricating Greases. *J. Am. Soc. Lubn. Eng.* **1977**, *33*, 133–138.
- (33) Uzu, Y. The Phase Behavior and Colloidal Structure of Lithium Stearate in Hydrocarbons. *J. Jpn. Oil Chem. Soc. (Yukagaku)* **1975**, *24*, 261–264.
- (34) Grahame, D. A. S.; Olouson, C.; Lam, R. S. H.; Pedersen, T.; Borondics, F.; Abraham, S.; Weiss, R. G.; Rogers, M. A. Influence of chirality on the modes of self-assembly of 12-hydroxystearic acid in molecular gels of mineral oil. *Soft Matter* **2011**, *7*, 7359–7365.
- (35) Fiero, G. W. *J. Am. Pharm. Assoc.* **1940**, *29*, 502–505.

- (36) Boner, C. J. *Manufacture and Application of Lubricating Greases*; Reinhold: New York, 1960.
- (37) Terech, P.; Rodriguez, V.; Barnes, J. D.; McKenna, G. B. Organogels and Aerogels of Racemic and Chiral 12-Hydroxyoctadecanoic Acid. *Langmuir* **1994**, *10*, 3406–3418.
- (38) Tachibana, T.; Mori, T.; Hori, K. Chiral Mesophases of 12-Hydroxyoctadecanoic Acid in Jelly and in the Solid State. I. A New Type of Lyotropic Mesophase in Jelly with Organic Solvents. *Bull. Chem. Soc. Jpn.* **1980**, *53*, 1714–1719.
- (39) Terech, P. 12D-Hydroxyoctadecanoic Acid Organogels: A Small Angle Neutron Scattering Study. *J. Phys. II* **1992**, 2181–2195.
- (40) Hayes, I. C.; Stone, A. J. An Intermolecular Perturbation Theory for the Region of Moderate Overlap. *Mol. Phys.* **1984**, *53*, 83–105.
- (41) Bondi, A. van der Waals Volumes and Radii. *J. Phys. Chem.* **1964**, *68*, 441–451.
- (42) Mantina, M.; Chamberlin, A. C.; Valero, R.; Cramer, C. J.; Truhlar, D. G. Consistent van der Waals Radii for the Whole Main Group. *J. Phys. Chem. A* **2009**, *113*, 5806–5812.
- (43) Tachibana, T.; Mori, T.; Hori, K. Chiral mesophases of 12-hydroxyoctadecanoic acid in jelly and in the solid state. I. A new type of lyotropic mesophase in jelly with organic solvents. *Bull. Chem. Soc. Jpn.* **1980**, *53*, 1714–1719.
- (44) Ostuni, E.; Kamaras, P.; Weiss, R. G. Novel X-ray Method for In Situ Determination of Gelator Strand Structure: Polymorphism of Cholesteryl Anthraquinone-2-carboxylate. *Angew. Chem., Int. Ed.* **1996**, *35*, 1324–1326.
- (45) Mallia, A.; George, M.; Blair, D. L.; Weiss, R. G. Robust Organogels from Nitrogen-Containing Derivatives of (R)-12-Hydroxystearic Acid as Gelators: Comparisons with Gels from Stearic Acid Derivatives. *Langmuir* **2009**, *25*, 8615–8625.
- (46) Raghavan, S. R.; Cipriano, B. H. in Weiss, R. G.; Terech, P. (Eds.) *Molecular Gels: Materials with Self-Assembled Fibrillar Networks*, Springer, Dordrecht, 2006, chap 8.
- (47) Weiss, R. G.; Terech, P. (Eds.) *Molecular Gels: Materials with Self-Assembled Fibrillar Networks*, Springer, Dordrecht, 2006.
- (48) Kitaigorodsky, A. I. *Molecular Crystals and Molecules*; Academic Press: New York, 1973, p 335.
- (49) Marton, L.; McBain, J. W.; Vold, R. D. An Electron Microscope Study of Curd Fibers of Sodium Laurate. *J. Am. Chem. Soc.* **1941**, *63*, 1990–1993.
- (50) Zana, R. Partial Phase Behavior and Micellar Properties of Tetrabutylammonium Salts of Fatty Acids: Unusual Solubility in Water and Formation of Unexpectedly Small Micelles. *Langmuir* **2004**, *20*, 5666–5668.
- (51) Novales, B.; Navilles, L.; Axelos, M.; Nallet, I.; Douliez, J.-P. Self-Assembly of Fatty Acids and Hydroxy Derivative Salts. *Langmuir* **2008**, *24*, 62–68.
- (52) Lin, Y.; Kachar, B.; Weiss, R. G. Liquid-Crystalline Solvents as Mechanistic Probes. Part 37. Novel Family of Gelators of Organic Fluids and the Structure of Their Gels. *J. Am. Chem. Soc.* **1989**, *111*, 5542–5551.
- (53) Furman, I.; Weiss, R. G. Factors influencing the formation of thermally reversible gels comprised of cholesteryl 4-(2-anthryloxy)-butanoate in hexadecane, 1-octanol, or their mixtures. *Langmuir* **1993**, *9*, 2084–2088.
- (54) Davey, R. J.; Garside, J. *From Molecules to Crystallizers*; Oxford University Press: New York, 2000; Chapter 2 and references cited therein.
- (55) Rogers, M. A.; Marangoni, A. G. Non-isothermal nucleation and crystallization of 12-hydroxystearic acid in vegetable oils. *Cryst. Growth Des.* **2008**, *8*, 4596–4601.
- (56) Abraham, S.; Lan, Y.; Lam, R. S. H.; Grahame, D. A. S.; Kim, J. J. H.; Weiss, R. G.; Rogers, M. A. Influence of the Hydroxy Position in Racemic Hydroxyoctadecanoic Acids on the Crystallization Kinetics and Activation Energies of Gels and Dispersions in Mineral Oil. *Cryst. Growth Des.* **2012**, *12*, 5497–5504.
- (57) The molecular lengths of the n-KSA were calculated using the MM2 program of CS Chem3D Std software.